Single-cell analysis of bone marrow CD8$^+$ T cells in Myeloid Neoplasms predicts response to treatment with Azacitidine

Authors:

Athanasios Tasis[1,2], Nikos E. Papaioannou[3,*], Maria Grigoriou[1,4,*], Nikolaos Paschalidis[4,*], Katerina Loukogiannaki[4], Anastasia Filia[1,4], Kyriaki Katsiki[1], Eleftheria Lamprianidou[2], Vasileios Papadopoulos[2], Christina Maria Rimpa[1,2], Antonios Chatzigeorgiou[5], Ioannis P. Kourtzelis[6], Petroula Gerasimou[7], Ioannis Kyprianou[7], Paul Costeas[7], Panagiotis Liakopoulos[8], Konstantinos Liapis[2], Petros Kolovos[8], Triantafyllos Chavakis[9,10], Themis Alissafi[3,11], Ioannis Kotsianidis[2,*], Ioannis Mitroulis[1,2,9, 10,*,#]

Affiliations:

[1]Translational Research and Laboratory Medicine Unit, First Department of Internal Medicine, University Hospital of Alexandroupolis, Democritus University of Thrace; Alexandroupolis, Greece

[2]Department of Hematology, University Hospital of Alexandroupolis, Democritus University of Thrace; Alexandroupolis, Greece

[3]Laboratory of Immune Regulation, Center of Basic sciences, Biomedical Research Foundation Academy of Athens; Athens, Greece

[4]Laboratory of Autoimmunity and Inflammation, Center of Clinical, Experimental Surgery and Translational Research, Biomedical Research Foundation Academy of Athens; Athens, Greece

[5]Department of Physiology, Medical School, National and Kapodistrian University of Athens; Athens, Greece

[6]Hull York Medical School, York Biomedical Research Institute, University of York; York, United Kingdom

[7]Molecular Hematology-oncology, Karaiskakio Foundation, Nicosia, Cyprus

[8]Department of Molecular Biology and Genetics, Democritus University of Thrace, 68100 Alexandroupolis, Greece.

[9] Institute for Clinical Chemistry and Laboratory Medicine, University Hospital and Faculty of Medicine Carl Gustav Carus of TU Dresden; Dresden, Germany
[10] National Center for Tumor Diseases, Partner Site Dresden, 01307 Dresden, Germany
[11] Laboratory of Biology, School of Medicine; Athens, Greece

* These authors contributed equally to this work

Corresponding author: Ioannis Mitroulis, MD, PhD, Email: imitroul@med.duth.gr

Running Title:

Single-cell analysis of $CD8^+$ T cells in MDS

Data Sharing Statement

The authors state that all data supporting this study are available in the main text or the supplementary material. The raw scRNA-sequencing data for this study have been deposited in the NCBI's Gene Expression Omnibus repository and are accessible through accession number GSE250077. All other raw data can be provided by the authors upon reasonable request.

Key-points

- The frequency of bone marrow $CD57^+CXCR3^+$ $CD8^+$ T cell subset predicts response to azacitidine in MDS and AML patients.
- scRNA-seq analysis linked IFN pathway and TGF-β pathway signature in $CD8^+$ T cells with response and failure to treatment, respectively.

Abstract

Treatment with hypomethylating agents (HMA), and specifically azacitidine (AZA), is the standard of care for patients with higher-risk myelodysplastic syndromes (MDS) and acute myeloid leukemia (AML) that are not eligible to receive intensive chemotherapy. Despite research efforts, it is not possible to predict response to treatment with HMA. In this study, we aimed to identify immune cell signatures in the bone marrow (BM) associated with treatment outcomes. By employing mass cytometry, we performed an in-depth immunophenotypic analysis in BM samples deriving from patients with myeloid neoplasms prior to treatment initiation. We identified an increased pre-treatment frequency of a $CD8^+$ T cell subset, characterized as $CD57^+CXCR3^+CCR7^-CD45RA^+$, in patients with MDS and AML who did not respond to treatment with AZA, compared to responders. Furthermore, an increased baseline frequency (>29%) of $CD57^+CXCR3^+CD8^+$ T cells was correlated with poor overall survival. We further engaged scRNA-seq to assess the transcriptional profile of BM $CD8^+$ T cells from treatment-naïve patients with MDS and AML, to identify molecular signatures in $CD8^+$ T subpopulations associated with favorable outcomes. Response to treatment was positively associated with enrichment of IFN-mediated pathways coupled with enhanced cytotoxic signature, whereas enrichment of the TGF-β signaling pathway was observed in cell clusters from non-responders. Together, this study identified a specific $CD57^+CXCR3^+$ $CD8^+$ T cell population with predictive value in patients with MDS and AML treated with AZA and characterized molecular signatures in $CD8^+$ T cells linked to cytokine signaling that were associated with treatment outcomes.

Main Text:

INTRODUCTION

Myeloid neoplasms encompass a diverse group of clonal disorders, including myelodysplastic syndromes (MDS), chronic myelomonocytic leukemia (CMML) and acute myeloid leukemia (AML), which share common features in their pathobiology.[1] While genetic alterations and epigenetic modifications play a role in the development of myeloid neoplasms, the interaction between clonal and immune cells is crucial.[2–5] Despite being clonal diseases originating from hematopoietic stem cell progenitors, there is compelling evidence from human and animal studies indicating that the interplay between clonal cells and the bone marrow (BM) microenvironment plays a significant role in the development and progression of MDS and CMML.[6–12]

T lymphocytes, and especially $CD8^+$ T cells play, a crucial role in the regulation of tumor microenvironment.[13] Aberrant functionality of $CD8^+$ T cells has been observed in patients with myeloid neoplasms compared to healthy individuals.[14,15] The impaired functionality of $CD8^+$ T lymphocytes within the tumor microenvironment constitutes an important target for immunotherapeutic interventions.[16–21] Nevertheless, the role of T cells in disease progression and response to treatment in myeloid neoplasms remains largely unknown.

To date, the most utilized tool for the stratification of MDS patients into risk groups is the Revised International Prognostic Scoring System (IPSS-R), based on clinical and laboratory parameters.[22] The recently developed Molecular IPSS (IPSS-M) includes also mutational data.[23] The standard of care for patients with higher-risk MDS (HR-MDS) and non-proliferating CMML, as well as patients with secondary AML, who are not eligible for intensive chemotherapy, is treatment with hypomethylating agents (HMA) like azacitidine (AZA).[24–27]

However, not all patients exhibit a favorable response, and there is a significant risk of relapse.[28,29] Additionally, molecular predictors of response to HMA and the precise mechanism of action of this drug are not well-defined. The exact genetic and cellular processes through which HMA exerts its effects are still being studied,[30] whereas there are no therapeutic approaches to overcome resistance to this treatment.[31]

To address whether immune cells in the BM play a role in disease progression of myeloid neoplasms and in the prediction of the response to treatment, we engaged a systematic approach to study the immune landscape of BM samples from patients with myeloid neoplasms prior to treatment initiation. We performed mass cytometry (CyTOF) for the immunophenotypic characterization of immune cell populations in the BM. Based on this analysis, we then focused on $CD8^+$ T cells and performed single-cell RNA sequencing (scRNA-seq), to address the molecular signature in $CD8^+$ T cell subsets that are linked to response to treatment with AZA.

MATERIALS AND METHODS

A comprehensive description of the methods is given in supplemental Methods.

Study patients

BM samples were collected from patients with lower-risk (LR)-MDS, HR-MDS (subtypes Increased Blasts (IB)1 and IB2), AML and CMML-2 before treatment initiation. Detailed demographic and clinical data are presented in Table 1. The study was approved by the Ethics Committee of the University Hospital of Alexandroupolis, under the reference number (877/23-10-2019). All patients provided informed written consent in accordance with the principles outlined in the Declaration of Helsinki.

Mass cytometry and data analysis

High-dimensional immunophenotyping of bone marrow mononuclear cells (BMMCs) was performed with mass cytometry using established and validated workflows from previous studies.[32,33] We employed the Maxpar Direct Immune Profiling Assay (MDIPA) (Standard Biotools) (Supplemental Table 1).[34] Acquisition was performed using a Helios™ system. Data analysis was performed on $CD45^+$ cells. FlowSOM clustering analysis and dimensionality reduction via tSNE were carried out in the R programming environment (version 4.1.0), as previously described.[33] For targeted analysis of T cell populations, Cytobank was used.

scRNA-seq and data processing

Sorted cells were resuspended, combined by three per well of the Chromium Next GEM Chip G (10X Genomics) and loaded onto the Chromium Controller (10X Genomics). Samples were processed for single-cell encapsulation, cDNA and cell multiplexing library generation using the Chromium Next GEM Single Cell 3 Reagent Kits v3.1 (Dual Index) (10X Genomics). The constructed libraries were sequenced on an NovaSeq 6000 sequencer. The 10X Genomics Cell Ranger multi v7.1.0 pipeline, was used to map the sequencing reads to the human genome (GRCh38) and generate the gene expression and feature barcode matrices.

RESULTS

Immunophenotypic analysis of BM immune cell populations

To study the immune cell compartment, we performed deep immunophenotyping using CyTOF in BM samples from patients with LR-MDS, HR-MDS, AML and CMML collected before treatment initiation. Multidimensional scaling analysis revealed a separation of samples derived from patients with MDS and AML compared to CMML based on dimension 2 (Figure 1A). Untargeted cluster analysis resulted in the identification of 14 clusters of cells (Figure 1B-C). We observed a significantly decreased frequency of cells in the cluster of $CD4^+$ T cells (CD4 T1) and B cells in patients with CMML, with a respective increase in the frequency of monocytic cells of myeloid cluster 2, characterized by the expression of CD11c, CD14 and CD38 (Figure 1D). We further evaluated the expression of the chemokine receptors C-C chemokine receptor 4 (CCR4), CCR6, CCR7 and C-X-C Motif Chemokine Receptor 3 (CXCR3), CD161 and CD294 within the T cell clusters (Supplemental Figure 1). We observed increased expression of CXCR3 on cells

from patients with AML and CMML compared to MDS patients in the CD4 T2, CD8 T1 and CD8 T2 clusters (Figure 1E).

Based on these findings, we then focused on $CD4^+$ and $CD8^+$ T cells and performed an untargeted cluster analysis on $CD3^+CD4^-CD8^+$ (Figure 2) and $CD3^+CD4^+CD8^-$ T cells (Supplemental Figure 2). We identified 10 clusters of $CD8^+$ T cells (Figure 2A). We observed a significant decreased frequency of cells within cluster 1 in samples from patients with LR-MDS and HR-MDS compared to AML and CMML (Figure 2B), which included terminal effector cells ($CCR7^-CD45RA^+$), expressing CD57 and CXCR3 (Figure 2C). We also identified an additional cluster (cluster 2) of terminal effector cells ($CCR7^-CD45RA^+$), that did not express CD57 and CXCR3, and did not show any difference among the groups (Figure 2B-C). Additionally, the expression of CXCR3 within cluster 1 was higher in cells from patients with AML and CMML compared to patients with HR-MDS (Figure 2D). Similar analysis on $CD4^+$ T cells did not reveal any difference in the frequency of the generated clusters (Supplemental Figure 2).

Based on these findings, we further engaged flow cytometry in BM cells from an additional cohort of patients, focusing on the frequency of $CD3^+CD8^+CD57^+CXCR3^+$ T cells (Figure 2E-F). We included samples from eight patients that were also analyzed with CyTOF, to compare the two methods. We observed that the frequency of this cell population within $CD8^+$ T cells was increased in patients with AML and CMML compared to LR- and HR-MDS (Figure 2F), being in line with the findings from the unsupervised analysis of data derived from CyTOF.

The proportion of $CD57^+CXCR3^+$ $CD8^+$ T cells is associated with the response to AZA

We next assessed whether the proportion of $CD57^+CXCR3^+$ within the $CD8^+$ T cell population before treatment initiation with HMA was associated with response to treatment. Univariate analysis revealed that a decreased percentage of $CD57^+CXCR3^+$ $CD8^+$ T cells is associated with better response (Supplemental Table 2). The frequency of this cell subset was significantly increased in patients with HR-MDS and AML that did not respond to treatment, whereas no difference was observed in patients with CMML (Figure 3A). Next, utilizing the CyTOF data, we performed unsupervised cluster analysis of $CD3^+CD4^-CD8^+$ T cells in responders and non-responders to AZA patients with MDS and AML, which resulted in the identification of 6 cell clusters (Figure 3B). We observed an increased frequency of cluster 3 in non-responders (Figure 3B and D), a cluster of $CCR7^-CD45RA^+$ effector cells characterized by the expression of CD57 and CXCR3 (Figure 3C). Conversely, we observed an increased frequency of cluster 6 in responders, characterized by naive/memory markers CD28, CD27, CCR7, CD127 (Figure 3C-D). On the other hand, there was no difference between responders and non-responders in the analysis of $CD3^+CD8^-CD4^+$ T cells (Supplemental Figure 3).

We further evaluated whether the frequency of the $CD57^+CXCR3^+$ $CD8^+$ T cell subset was associated with survival. To do so, optimal $CD57^+CXCR3^+$ cut-off was determined at >29% by transformation of scale variable to binary one through optimal scaling. We observed that patients with ≤29% $CD57^+CXCR3^+$ $CD8^+$ T cells had better overall survival (OS) (Figure 3E). When patients with HR-MDS, AML and CMML were evaluated separately, we observed that this cut-off value could be applied to patients with HR-MDS and AML but not to patients with CMML (Figure 3F). Thereafter, we aimed to assess the applicability of this cut-off in predicting response to treatment with AZA. Patients with HR-MDS and AML and ≤29% $CD57^+CXCR3^+$ $CD8^+$ T cells demonstrated higher rates of response to AZA (Figure 3G). In contrast, the percentage of

$CD57^+CXCR3^+$ $CD8^+$ T cells was not associated with response to treatment in patients with CMML (Figure 3G). Together, these findings suggest that an increased frequency of the $CD57^+CXCR3^+$ $CD8^+$ T cell subset is associated with treatment failure and worse survival in patients with MDS and AML treated with AZA.

Association between mutational status and frequency of $CD57^+CXCR3^+$ $CD8^+$ T cells

We further investigated whether there is a connection between mutational burden, type of mutations, and the frequency of $CD57^+CXCR3^+$ $CD8^+$ T cells. No difference was found in the frequency of this cell population when patients were categorized based on the oncogenic mutations (Supplemental Figure 4A), whereas no single mutation was associated with an increased frequency (>29%) of the $CD57^+CXCR3^+$ $CD8^+$ T cell subset (Supplemental Figure 4B). Furthermore, the number of oncogenic mutations was not significantly altered in patients with >29% $CD57^+CXCR3^+$ $CD8^+$ T cells compared to patients with a lower frequency (≤29%) (Supplemental Figure 4C), and no specific group of oncogenic mutations was associated with the frequency of $CD57^+CXCR3^+$ T cells (Supplemental Figure 4D).

Single-cell transcriptomes of $CD8^+$ T cells are associated with treatment outcome

We next sought to assess the molecular signature of BM $CD8^+$ T cells from patients with MDS and AML at the single cell level, to identify molecular signatures in specific $CD8^+$ T cell subpopulations associated with a favorable outcome. scRNA-seq was performed in sorted BM $CD8^+$ T cells from patients with HR-MDS (n=4) and AML (n=5). We obtained transcriptomes of 28,449 cells in total. Based on unsupervised clustering, cells were partitioned in 11 clusters (Figure 4A), which were characterized according to the gene expression of markers associated

with T cell phenotype,[35] including naive/memory markers (*CCR7*, *IL7R*, *SELL*, *CD27*, *CD28*, *CD44*), cytotoxic markers (*GZMA*, *GZMB*, *GZMK*, *PRF1*, *CX3CR1*, *NKG7*, *HOPX*, *KLRG1)*, cell cycle genes (*MKI67*, *CCNB2)*, the transcription factors (TFs) *LEF1*, *EOMES* and *TCF7*, the cytokine *IFNG*, and the cell surface markers *ITGA1*, *CD69* and *CCR6* (Figure 4B-C). We identified clusters of cells characterized by the expression of *GZMK* (cluster 0), and *EOMES*, *KLRG1* and *GZMK* (cluster 1), previously characterized as pre-dysfunctional.[35,36] We further identified two clusters of cytotoxic $CD8^+$ T lymphocytes, clusters 2 (CTL_1) and 4 (CTL_2), based on the expression of *GZMA*, *GZMB* and *PRF1*.[37] Clusters 1, 2 and 4 were the clusters with the highest frequency of cells expressing *B3GAT1*, the gene that encodes CD57 (Supplemental Figure 5). We identified a cluster of memory-like cells, characterized by the expression of *IL7R* and low expression of *CCR7*, *SELL*, *CD27* (cluster 3), a cluster of naive-like cells, expressing *CCR7*, *SELL*, *CD27* and the TFs *TCF7* and *LEF1*[38] (cluster 5), a cluster characterized by the expression of *CCR6* (cluster 6) and a cluster characterized by the highest expression of *CD44* (cluster 7) (Figure 4B-C). Cluster 8 included cells expressing *ITGA1* and *ITGAE* (Figure 4D), previously described as resident memory cells (cluster 8),[38–40] and cluster 9 included cytotoxic cells expressing *IFNG*, *GZMK* and *NKG7*. We did not observe significant expression of genes associated with exhaustion, such as *PDCD1*, *LAG3*, *HAVCR2*, *ENTPD1* or *CTLA4*[35] or a cluster of cells characterized by the expression of such genes (Figure 4B; Supplemental Figure 6). Finally, a cluster of proliferating T cells (cluster 10) was identified (Figure 4B-C). Top differentially expressed genes (DEGs) for each cell cluster are depicted in Figure 4D. We further engaged a previously reported cytotoxic score[41] to confirm the enhanced cytotoxicity of cells in clusters 2 (CTL_1), 4 (CTL_2) and 9 (*IFNG*) (Figure 4E) and a cell cycle score[41] to confirm the increased proliferation activity of cells in cluster 10 (Proliferative) (Figure 4F). We next

investigated the trajectories that cells traverse during T cell differentiation, using naïve-like cells (cluster 5), as a starting point (Figure 4G). Based on this analysis, we observed that cells from clusters 1 (*EOMES*), 2 (CTL_1) and 7 (*CD44)* are composed of cells most differentiated cells (Figure 4G). Regarding the trajectories that lead to these clusters, we identified one trajectory that derives from cluster 0 (*GZMK*) and leads to clusters 2 (CTL_1) and 7 (*CD44)* through cluster 1 (*EOMES*) and two other trajectories that derive from cluster 0 (*GZMK*) and lead to 2 (CTL_1) through cluster 4 (CTL_2) (Figure 4G).

Single-cell transcriptomes of CD8$^+$ T cells are associated with treatment outcome

We next sought to investigate the molecular signatures in CD8$^+$ T cell subpopulations associated with response to AZA (Figure 5A). We did not observe any statistically significant difference in the cluster abundance in patients that achieved complete remission (CR) after treatment with AZA (n=2 patients with HR-MDS, 7,571 cells; n=2 patients with AML, 6,096 cells) and patients that failed (FAIL) to treatment (n=2 patients with HR-MDS, 8,026 cells; n=3 patients with AML, 6,756 cells) (Figure 5B), except from an increased abundancy of cluster 10 (Proliferative) in the CR group (Supplemental Figure 7).

Pathway analysis was performed, and DEGs upregulated in the CR group were associated with IFN response in all clusters (Figure 5C). To this direction, increased expression of the IFN-responsive genes *MT2A*, *BST2*, *STAT1* and *IRF2* was observed in the CR group (Figure 5D). We then focused on specific clusters, and we used a score that derives from the expression of interferon stimulated genes (ISG signature).[42] We observed higher ISG signature score in the CR group in cluster 0 (*GZMK*), which was associated with increased expression of the IFN-responsive genes *CCL5*, *MT2A*, *BST2*, *CD74*, *GZMA*, *PSME1*, *PSME2*, *CD69*, *VAMP8* and

TXNIP (Figure 5E). Similarly, increased expression of *HLA-DRB1*, *MT2A*, *BST2*, *CD74*, *TXNIP*, *GZMA*, *PSME1*, *PSME2*, *CD69*, *PTPN2*, *IRF2*, *STAT1*, *SOCS1* and *KLRK1* was observed in cluster 1 (*EOMES*) (Figure 5F). Regarding the cytotoxic clusters 2 (CTL_1) (Figure 5G; Supplemental Figure 8A) and 4 (CTL_2) (Figure 5H; Supplemental Figure 8B), higher ISG signature and increased expression of the genes *IFITM2*, *MT2A*, *BST2*, *STAT1*, *GZMA*, *PSME1*, *PSME2* and *CD69* was detected in cells from the CR group from both clusters.

Pathway analysis of DEGs upregulated in the FAIL group demonstrated that cells from the clusters 0 (*GZMK*), 1 (*EOMES*), 2 (CTL_1), 3 (Memory), 4 (CTL_2), 5 (Naïve), 6 (*CCR6*) and 8 (Trm) were enriched for DEGs associated with TNF signaling (Figure 6A; Supplemental Figure 9). Moreover, cells from the cytotoxic clusters 2 (CTL_1), 4 (CTL_2), 9 (*IFNG*) and clusters 3 (Memory), 6 (*CCR6*) and 7 (*CD44*) were enriched for DEGs of the TGF-β signaling pathway (Figure 6A). Specifically for cluster 2 (CTL_1), there was higher TGF-β signature score in the FAIL group and increased expression of *TFGB1*, *SMURF2*, *SMAD7*, *SKI*, *SKIL* (Figure 6B; Supplemental Figure 8A), whereas for cluster 4 (CTL_2) the higher TGF-β signature score was associated with increased expression of *TFGB1*, *ARID4B*, *SMAD7*, *SKI*, *SKIL* and *SMURF2* (Figure 6C; Supplemental Figure 8B). Since TGF-β signaling has been previously associated with decreased cytotoxicity,[43] we further used the cytotoxic signature score (Figure 6D) to address whether the TGF-β signature is associated with decreased cytotoxic activity in CTL clusters in the FAIL group. We observed higher cytotoxic score in the CR group in cluster 2 (CTL_1), which was associated with the enhanced expression of *GZMA*, *GZMB*, *CX3CR1* and *CCND3* (Figure 6E) and in cluster 4 (CTL_2), which was associated with enhanced expression of *FGFBP2*, *GZMA*, *GZMB*, *GZMH*, *CCND3*, *C1orf162* and *CX3CR1* (Figure 6F).

Cytokines act together with transcription factors (TFs) to regulate T cell fate and functionality.[44] To study the TFs that could act as possible regulators of the transcriptomic alterations observed in responders to AZA compared to non-responders, TF regulatory network analysis was performed using SCENIC,[45] which resulted in the identification of 11 clusters-regulons (Figure 7A). We observed that regulon 5 was enriched with cells from the CR group of patients, whereas regulon 7 was enriched with cells from the FAIL group (Figure 7B-C). Regulon cluster 5 was characterized by IRF7-, CHURC1-, NFYB- and RFXANK-regulated networks (Figure 7D) and was enriched mainly with cells from cluster 4 (CTL_2) (Supplemental Figure 10). On the other hand, regulon 7 was characterized by the NFKB2-, REL-, RELB-, CREM- and NFKB1-regulated networks (Figure 7D) and it was enriched with cells from cluster 0 (*GZMK*) and cluster 1 (*EOMES*) (Supplemental Figure 10), previously described as pre-dysfunctional cells.[35,36] Differential TF activity analysis between the two groups of patients within regulon 5, predicted that the activity of the TFs IRF2, IRF9 and STAT1 was increased in the CR group and the activity of RELB, REL, NFKB2, NFKB1 and SMAD3 was increased in the FAIL group (Figure 7E). Similar analysis within regulon 7, predicted increased activity for IRF2 and STAT1 and decreased activity for NFKB1 in cells derived from the CR group (Figure 7F). Taken together, the TF regulatory network analysis further supports that BM $CD8^+$ T cells in the CR group are targeted by TFs associated with IFN signaling, whereas TFs linked to TGF-β and TNF signaling target $CD8^+$ T cells in the FAIL group.

DISCUSSION

Herein, we provide a systemic analysis at the single cell level of $CD8^+$ T cells derived from the BM immune microenvironment of patients with myeloid neoplasia. We specifically focused on the identification of specific immunophenotypic, and molecular signatures associated with the outcome of AZA treatment.

Deep immunophenotyping with CyTOF demonstrated that patients with HR-MDS and AML who did not respond to treatment with AZA exhibited increased pre-treatment levels of the $CD57^+CXCR3^+$ $CD8^+$ T cell subset compared to responders, while a frequency of $CD57^+CXCR3^+$ $CD8^+$ T cells of more than 29% prior to initiation of treatment was associated with worse OS. Hence, our findings demonstrate a significant correlation between elevated pre-treatment frequencies of the $CD57^+CXCR3^+$ $CD8^+$ T cell subset and unfavorable outcome in patients with HR-MDS and AML under treatment with AZA.

The expression of CD57 by $CD8^+$ T cells, coupled with the absence of CD28 expression, characterizes a senescent-like phenotype, linked to chronic immune activation in several disorders.[46–49] These $CD57^+CD28^-$ $CD8^+$ T cells are antigen specific effector cells that have limited proliferation capacity, due to their advanced differentiation stage.[50,51] Previous studies demonstrated increased levels of $CD57^+CD28^-$ $CD8^+$ T cells in patients with MDS and AML compared to healthy individuals.[15,52] CXCR3, on the other hand, is expressed on Th1-$CD4^+$ T cells[53] and effector $CD8^+$ T cells[54] and is considered crucial for the recruitment of T cells to inflammatory sites.[54–56] The expression of CXCR3 on $CD8^+$ T cells has been associated with changes in the equilibrium from memory towards effector cell populations.[57,58] Interestingly, recent studies engaging scRNA-seq in $CD8^+$ T cells isolated from patients with cancer have described cells expressing *CXCR3* together with *GZMK* and *EOMES* as a pre-dysfunctional cell

population.[36,59] In this study, we demonstrate for the first time that enhanced frequency of the $CD8^+$ T subset $CD57^+CXCR3^+$ is linked to adverse outcomes in patients with HR-MDS and AML treated with AZA.

Recent findings indicate that the immune system, specifically $CD4^+$ and $CD8^+$ T cells, is affected and plays a critical role in the response to AZA,[60–62] a DNA hypomethylating agent which has emerged as a standard treatment option for patients who are ineligible for intensive chemotherapy.[63–65] In this study, we observed that patients that did not respond to AZA treatment were characterized by increased levels of a $CD57^+CXCR3^+$ $CD8^+$ T cells, prior to the initiation of AZA treatment. It has been recently demonstrated that the accumulation of senescent-like $CD8^+CD57^+$ T cells is negatively associated with the response to chemotherapy and checkpoint blockade immunotherapy in AML patients.[66] Interestingly, utilizing *in vitro* studies, it was shown that patient-derived senescent-like T cells were not able to sufficiently eliminate autologous AML-blasts when compared to their non-senescent $CD8^+$ T cell counterparts, providing evidence for their limited ability to clear leukemic cells.[66] To the same direction, we demonstrate that increased pre-treatment frequency of BM $CD57^+CXCR3^+$ $CD8^+$ T cells is associated with poor OS and response to AZA treatment.

Based on our findings from immunophenotyping, we engaged scRNA-seq analysis to investigate $CD8^+$ T cells from responders and non-responders to AZA treatment. A significant enrichment of the TGF-β signaling pathway was observed in cytotoxic clusters (CTL_1 and CTL_2) of non-responders. This pathway has been associated with suppression of cytotoxicity, tumor evasion and poor outcomes.[67] In line with this, non-responders displayed decreased cytotoxic signature within the same clusters. Interestingly, Luspatercept, a TGF-β inhibitor, has been approved by the FDA as a line of treatment for patients with anemia and lower-risk myelodysplastic

syndromes with ring sideroblasts.[68,69] Studies have shown that Luspatercept can sufficiently stimulate erythropoiesis resulting in transfusion independence, while also significantly extending the time to AML progression.[70] To this direction, it could be worthwhile considering the potential benefits of combined treatment with AZA and TGF-β inhibitors for patients with HR-MDS and AML.

On the other hand, responders exhibited a significant enrichment of pathways associated with IFN response, across many BM $CD8^+$ T cell clusters. Type I and II Interferons play a crucial role in immune activation during anti-tumor responses.[71–73] Notably, there is evidence indicating that AZA exerts its effects in an IFN-dependent manner by increasing the production of IFN-γ,[74] activating type I Interferon signaling,[75–77] as well as upregulating the expression of Interferon Stimulated Genes (ISGs), all of which aid in the rejuvenation of the anti-tumor immunity.[77,78] Taken together, our findings suggest that the balance between TGF-β and IFN signaling in CTLs within the BM microenvironment may regulate their anti-tumor effect, affecting the response to treatment.

Immunotherapies based on immune checkpoint blockade (ICB) have revolutionized the field of oncology, especially in the case of solid tumors.[79–82] Many studies employing scRNA-seq in solid tumors demonstrated that $CD8^+$ T cells show a distinct molecular signature, indicative of an exhausted phenotype, which is associated with disease progression and treatment resistance,[41,83–85] thereby providing evidence supporting the effectiveness of ICB treatment in these patients. In contrast, ICB therapy in myeloid malignancies, including MDS and AML, has yielded limited results so far, while the risk of serious adverse events still remains.[86,87] Notably, our scRNA-seq analysis did not reveal any distinct $CD8^+$ T cell clusters with expression of genes related to a

dysfunctional/exhausted molecular signature. These findings support the clinical observations that ICB treatment might not be the optimal option for HR-MDS and AML treatment.

Taken together, this study provides important insights on the specific phenotypes and molecular signatures associated with effector T cell functionality of BM $CD8^+$ T cells that can inform prognosis in MDS and AML patients treated with AZA. To our knowledge, we studied for the first time, at the single cell level, the association between BM $CD8^+$ T cells and the outcome of AZA treatment in primary human samples of patients with myeloid neoplasia. Prospective studies in large cohorts are needed to evaluate whether the relative frequency of $CD8^+$ T cell subpopulations could be used in the prognostication of patients with myeloid neoplasms treated with hypomethylating agents.

Funding:

This study was supported by the Hellenic Foundation for Research and Innovation (HFRI) under the HFRI "Research Projects to Support Faculty Members & Researchers and Procure High-Value Research Equipment" grant (HFRI-FM17-452) and the General Secretariat for Research and Technology Management and Implementation Authority for Research, Technological Development, and Innovation Actions (MIA-RTDI) (grant T2EDK-02288, MDS-TARGET). TA and NEP are supported by the ERC under the European Union's Horizon 2020 research and innovation program (grant agreement no 947975 to T. Alissafi) and from the Hellenic Foundation for Research and Innovation (H.F.R.I.) under the "2nd Call for H.F.R.I. Research Projects to support Post-Doctoral Researchers" (Project Number: 166 to T. Alissafi) and the "Sub-action 1. Funding New Researchers – RRF: Basic Research Financing (Horizontal support for all Sciences) (Project number: 15014 to T. Alissafi). IPK is funded by the Academy of Medical Sciences (R2429101) and Rosetrees Trust (R2449101). TC is supported by the Deutsche Forschungsgemeinschaft (TRR332, project B4).

Authorship Contributions:

Conceptualization: AT, IK, IM

Methodology: AT, MG, NEP, NP, PC, TC, TA, IM

Investigation: AT, MG, KLO, AF, KK, EL, VP, AC, IPK, PG, PK, PL, IKY, KL

Visualization: AT, NEP, NP

Funding acquisition: IPK, TC, TA, IM

Project administration: IM

Supervision: IM

Writing – original draft: AT, IM

Writing – review & editing: AT, IPK, TC, IK, IM

Competing interests: Authors declare that they have no competing interests.

References

1. Arber DA, Orazi A, Hasserjian RP, et al. International Consensus Classification of Myeloid Neoplasms and Acute Leukemias: integrating morphologic, clinical, and genomic data. *Blood*. 2022;140(11):1200–1228.
2. Ogawa S. Genetics of MDS. *Blood*. 2019;133(10):1049–1059.
3. Itzykson R, Fenaux P. Epigenetics of myelodysplastic syndromes. *Leukemia*. 2014;28(3):497–506.
4. Fozza C, Crobu V, Isoni MA, Dore F. The immune landscape of myelodysplastic syndromes. *Crit Rev Oncol Hematol*. 2016;107:90–99.
5. Will B, Zhou L, Vogler TO, et al. Stem and progenitor cells in myelodysplastic syndromes show aberrant stage-specific expansion and harbor genetic and epigenetic alterations. *Blood*. 2012;120(10):2076–2086.
6. Balderman SR, Li AJ, Hoffman CM, et al. Targeting of the bone marrow microenvironment improves outcome in a murine model of myelodysplastic syndrome. *Blood*. 2016;127(5):616–625.
7. Kitagawa M, Yamaguchi S, Takahashi M, et al. Localization of Fas and Fas ligand in bone marrow cells demonstrating myelodysplasia. *Leukemia*. 1998;12(4):486–492.
8. Ferrer RA, Wobus M, List C, et al. Mesenchymal stromal cells from patients with myelodyplastic syndrome display distinct functional alterations that are modulated by lenalidomide. *Haematologica*. 2013;98(11):1677–1685.
9. Sarhan D, Wang J, Sunil Arvindam U, et al. Mesenchymal stromal cells shape the MDS microenvironment by inducing suppressive monocytes that dampen NK cell function. *JCI Insight*. 2020;5(5):130155.

10. Verstovsek S, Estey E, Manshouri T, et al. Clinical relevance of vascular endothelial growth factor receptors 1 and 2 in acute myeloid leukaemia and myelodysplastic syndrome. *Br J Haematol*. 2002;118(1):151–156.
11. Pronk E, Raaijmakers MHGP. The mesenchymal niche in MDS. *Blood*. 2019;133(10):1031–1038.
12. Chavakis T, Wielockx B, Hajishengallis G. Inflammatory Modulation of Hematopoiesis: Linking Trained Immunity and Clonal Hematopoiesis with Chronic Disorders. *Annual Review of Physiology*. 2022;84(1):183–207.
13. Verma NK, Wong BHS, Poh ZS, et al. Obstacles for T-lymphocytes in the tumour microenvironment: Therapeutic challenges, advances and opportunities beyond immune checkpoint. *EBioMedicine*. 2022;83:104216.
14. Knaus HA, Berglund S, Hackl H, et al. Signatures of CD8+ T cell dysfunction in AML patients and their reversibility with response to chemotherapy. *JCI Insight*. 2018;3(21):120974.
15. Radpour R, Riether C, Simillion C, et al. CD8+ T cells expand stem and progenitor cells in favorable but not adverse risk acute myeloid leukemia. *Leukemia*. 2019;33(10):2379–2392.
16. Liu X, Hoft DF, Peng G. Senescent T cells within suppressive tumor microenvironments: emerging target for tumor immunotherapy. *J Clin Invest*. 130(3):1073–1083.
17. Farhood B, Najafi M, Mortezaee K. CD8+ cytotoxic T lymphocytes in cancer immunotherapy: A review. *J Cell Physiol*. 2019;234(6):8509–8521.
18. Raskov H, Orhan A, Christensen JP, Gögenur I. Cytotoxic CD8+ T cells in cancer and cancer immunotherapy. *Br J Cancer*. 2021;124(2):359–367.

19. Huang Y, Jia A, Wang Y, Liu G. CD8+ T cell exhaustion in anti-tumour immunity: The new insights for cancer immunotherapy. *Immunology*. 2023;168(1):30–48.
20. Liu S, Sun Q, Ren X. Novel strategies for cancer immunotherapy: counter-immunoediting therapy. *J Hematol Oncol*. 2023;16(1):38.
21. Zhang J, He T, Xue L, Guo H. Senescent T cells: a potential biomarker and target for cancer therapy. *EBioMedicine*. 2021;68:103409.
22. Greenberg PL, Tuechler H, Schanz J, et al. Revised International Prognostic Scoring System for Myelodysplastic Syndromes. *Blood*. 2012;120(12):2454–2465.
23. Bernard E, Tuechler H, Greenberg PL, et al. Molecular International Prognostic Scoring System for Myelodysplastic Syndromes. *NEJM Evidence*. 2022;1(7):EVIDoa2200008.
24. Costa R, Abdulhaq H, Haq B, et al. Activity of azacitidine in chronic myelomonocytic leukemia. *Cancer*. 2011;117(12):2690–2696.
25. Platzbecker U, Fenaux P. Recent frustration and innovation in myelodysplastic syndrome. *Haematologica*. 2016;101(8):891–893.
26. Short NJ, Kantarjian H. Hypomethylating agents for the treatment of myelodysplastic syndromes and acute myeloid leukemia: Past discoveries and future directions. *Am J Hematol*. 2022;97(12):1616–1626.
27. Stomper J, Rotondo JC, Greve G, Lübbert M. Hypomethylating agents (HMA) for the treatment of acute myeloid leukemia and myelodysplastic syndromes: mechanisms of resistance and novel HMA-based therapies. *Leukemia*. 2021;35(7):1873–1889.
28. Nazha A, Komrokji RS, Garcia-Manero G, et al. The efficacy of current prognostic models in predicting outcome of patients with myelodysplastic syndromes at the time of hypomethylating agent failure. *Haematologica*. 2016;101(6):e224-227.

29. Prébet T, Gore SD, Esterni B, et al. Outcome of high-risk myelodysplastic syndrome after azacitidine treatment failure. *J Clin Oncol*. 2011;29(24):3322–3327.
30. Garcia-Manero G, Fenaux P. Hypomethylating agents and other novel strategies in myelodysplastic syndromes. *J Clin Oncol*. 2011;29(5):516–523.
31. Zhao G, Wang Q, Li S, Wang X. Resistance to Hypomethylating Agents in Myelodysplastic Syndrome and Acute Myeloid Leukemia From Clinical Data and Molecular Mechanism. *Front Oncol*. 2021;11:706030.
32. Vakrakou AG, Paschalidis N, Pavlos E, et al. Specific myeloid signatures in peripheral blood differentiate active and rare clinical phenotypes of multiple sclerosis. *Front Immunol*. 2023;14:1071623.
33. Nowicka M, Krieg C, Crowell HL, et al. CyTOF workflow: differential discovery in high-throughput high-dimensional cytometry datasets. *F1000Res*. 2017;6:748.
34. Bagwell CB, Hunsberger B, Hill B, et al. Multi-site reproducibility of a human immunophenotyping assay in whole blood and peripheral blood mononuclear cells preparations using CyTOF technology coupled with Maxpar Pathsetter, an automated data analysis system. *Cytometry B Clin Cytom*. 2020;98(2):146–160.
35. van der Leun AM, Thommen DS, Schumacher TN. CD8+ T cell states in human cancer: insights from single-cell analysis. *Nat Rev Cancer*. 2020;20(4):218–232.
36. Zhang L, Yu X, Zheng L, et al. Lineage tracking reveals dynamic relationships of T cells in colorectal cancer. *Nature*. 2018;564(7735):268–272.
37. Guo X, Zhang Y, Zheng L, et al. Global characterization of T cells in non-small-cell lung cancer by single-cell sequencing. *Nat Med*. 2018;24(7):978–985.

38. Clarke J, Panwar B, Madrigal A, et al. Single-cell transcriptomic analysis of tissue-resident memory T cells in human lung cancer. *J Exp Med*. 2019;216(9):2128–2149.
39. Szabo PA, Miron M, Farber DL. Location, location, location: Tissue resident memory T cells in mice and humans. *Sci Immunol*. 2019;4(34):eaas9673.
40. Kok L, Masopust D, Schumacher TN. The precursors of CD8+ tissue resident memory T cells: from lymphoid organs to infected tissues. *Nat Rev Immunol*. 2022;22(5):283–293.
41. Li H, van der Leun AM, Yofe I, et al. Dysfunctional CD8 T Cells Form a Proliferative, Dynamically Regulated Compartment within Human Melanoma. *Cell*. 2019;176(4):775-789.e18.
42. Chiche L, Jourde-Chiche N, Whalen E, et al. Modular transcriptional repertoire analyses of adults with systemic lupus erythematosus reveal distinct type I and type II interferon signatures. *Arthritis Rheumatol*. 2014;66(6):1583–1595.
43. Batlle E, Massagué J. Transforming Growth Factor-β Signaling in Immunity and Cancer. *Immunity*. 2019;50(4):924–940.
44. Kaech SM, Cui W. Transcriptional control of effector and memory CD8+ T cell differentiation. *Nat Rev Immunol*. 2012;12(11):749–761.
45. Aibar S, González-Blas CB, Moerman T, et al. SCENIC: single-cell regulatory network inference and clustering. *Nat Methods*. 2017;14(11):1083–1086.
46. Huff WX, Kwon JH, Henriquez M, Fetcko K, Dey M. The Evolving Role of CD8+CD28− Immunosenescent T Cells in Cancer Immunology. *International Journal of Molecular Sciences*. 2019;20(11):2810.
47. Tae Yu H, Youn J-C, Lee J, et al. Characterization of CD8(+)CD57(+) T cells in patients with acute myocardial infarction. *Cell Mol Immunol*. 2015;12(4):466–473.

48. Le Priol Y, Puthier D, Lécureuil C, et al. High cytotoxic and specific migratory potencies of senescent CD8+ CD57+ cells in HIV-infected and uninfected individuals. *J Immunol*. 2006;177(8):5145–5154.

49. Strioga M, Pasukoniene V, Characiejus D. CD8+ CD28- and CD8+ CD57+ T cells and their role in health and disease. *Immunology*. 2011;134(1):17–32.

50. Brenchley JM, Karandikar NJ, Betts MR, et al. Expression of CD57 defines replicative senescence and antigen-induced apoptotic death of CD8+ T cells. *Blood*. 2003;101(7):2711–2720.

51. Pangrazzi L, Reidla J, Carmona Arana JA, et al. CD28 and CD57 define four populations with distinct phenotypic properties within human CD8+ T cells. *Eur J Immunol*. 2020;50(3):363–379.

52. Epling-Burnette PK, Painter JS, Rollison DE, et al. Prevalence and clinical association of clonal T-cell expansions in Myelodysplastic Syndrome. *Leukemia*. 2007;21(4):659–667.

53. Yoon SH, Yun SO, Park JY, et al. Selective addition of CXCR3+CCR4-CD4+ Th1 cells enhances generation of cytotoxic T cells by dendritic cells in vitro. *Exp Mol Med*. 2009;41(3):161–170.

54. Groom JR, Luster AD. CXCR3 in T cell function. *Exp Cell Res*. 2011;317(5):620–631.

55. Maurice NJ, McElrath MJ, Andersen-Nissen E, Frahm N, Prlic M. CXCR3 enables recruitment and site-specific bystander activation of memory CD8+ T cells. *Nat Commun*. 2019;10(1):4987.

56. van der Voort R, Brandao C, Volman TJ, et al. CXCR3 Is Required for the Efficient Recruitment of Bone Marrow-Resident Memory T Cells to Inflamed Tissues,. *Blood*. 2011;118(21):3242.

57. Kurachi M, Kurachi J, Suenaga F, et al. Chemokine receptor CXCR3 facilitates CD8(+) T cell differentiation into short-lived effector cells leading to memory degeneration. *J Exp Med*. 2011;208(8):1605–1620.

58. Hu JK, Kagari T, Clingan JM, Matloubian M. Expression of chemokine receptor CXCR3 on T cells affects the balance between effector and memory CD8 T-cell generation. *Proceedings of the National Academy of Sciences*. 2011;108(21):E118–E127.

59. Yost KE, Satpathy AT, Wells DK, et al. Clonal replacement of tumor-specific T cells following PD-1 blockade. *Nat Med*. 2019;25(8):1251–1259.

60. Lamprianidou E, Kordella C, Kazachenka A, et al. Modulation of IL-6/STAT3 signaling axis in CD4+FOXP3− T cells represents a potential antitumor mechanism of azacitidine. *Blood Adv*. 2021;5(1):129–142.

61. Gang AO, Frøsig TM, Brimnes MK, et al. 5-Azacytidine treatment sensitizes tumor cells to T-cell mediated cytotoxicity and modulates NK cells in patients with myeloid malignancies. *Blood Cancer J*. 2014;4(3):e197.

62. Costantini B, Kordasti SY, Kulasekararaj AG, et al. The effects of 5-azacytidine on the function and number of regulatory T cells and T-effectors in myelodysplastic syndrome. *Haematologica*. 2013;98(8):1196–1205.

63. Zeidan AM, Fenaux P, Gobbi M, et al. Prospective comparison of outcomes with azacitidine and decitabine in patients with AML ineligible for intensive chemotherapy. *Blood*. 2022;140(3):285–289.

64. Döhner H, Estey E, Grimwade D, et al. Diagnosis and management of AML in adults: 2017 ELN recommendations from an international expert panel. *Blood*. 2017;129(4):424–447.

65. DiNardo CD, Jonas BA, Pullarkat V, et al. Azacitidine and Venetoclax in Previously Untreated Acute Myeloid Leukemia. *New England Journal of Medicine*. 2020;383(7):617–629.

66. Rutella S, Vadakekolathu J, Mazziotta F, et al. Immune dysfunction signatures predict outcomes and define checkpoint blockade–unresponsive microenvironments in acute myeloid leukemia. *J Clin Invest*. 2022;132(21):.

67. Thomas DA, Massagué J. TGF-beta directly targets cytotoxic T cell functions during tumor evasion of immune surveillance. *Cancer Cell*. 2005;8(5):369–380.

68. Fenaux P, Platzbecker U, Mufti GJ, et al. Luspatercept in Patients with Lower-Risk Myelodysplastic Syndromes. *New England Journal of Medicine*. 2020;382(2):140–151.

69. Fenaux P, Kiladjian JJ, Platzbecker U. Luspatercept for the treatment of anemia in myelodysplastic syndromes and primary myelofibrosis. *Blood*. 2019;133(8):790–794.

70. Platzbecker U, Santini V, Komrokji RS, et al. Analysis of Duration of Response, Exposure-Adjusted Safety and Progression to Acute Myeloid Leukemia (AML) for Patients with Lower-Risk Myelodysplastic Syndromes (LR-MDS) Receiving Luspatercept in the MEDALIST Study. *Blood*. 2021;138(Supplement 1):1524.

71. Overacre-Delgoffe AE, Chikina M, Dadey RE, et al. Interferon-γ Drives Treg Fragility to Promote Anti-tumor Immunity. *Cell*. 2017;169(6):1130-1141.e11.

72. Boukhaled GM, Harding S, Brooks DG. Opposing Roles of Type I Interferons in Cancer Immunity. *Annu Rev Pathol*. 2021;16:167–198.

73. Am G, Cj W, Daa V. Interferon-γ: teammate or opponent in the tumour microenvironment? *Nature reviews. Immunology*. 2022;22(3):.

74. Yano S, Ghosh P, Kusaba H, Buchholz M, Longo DL. Effect of Promoter Methylation on the Regulation of IFN-γ Gene During In Vitro Differentiation of Human Peripheral Blood T Cells into a Th2 Population. *The Journal of Immunology*. 2003;171(5):2510–2516.

75. Ohtani H, Ørskov AD, Helbo AS, et al. Activation of a Subset of Evolutionarily Young Transposable Elements and Innate Immunity Are Linked to Clinical Responses to 5-Azacytidine. *Cancer Research*. 2020;80(12):2441–2450.

76. Stone ML, Chiappinelli KB, Li H, et al. Epigenetic therapy activates type I interferon signaling in murine ovarian cancer to reduce immunosuppression and tumor burden. *Proceedings of the National Academy of Sciences*. 2017;114(51):E10981–E10990.

77. Chiappinelli KB, Strissel PL, Desrichard A, et al. Inhibiting DNA methylation causes an interferon response in cancer via dsRNA including endogenous retroviruses. *Cell*. 2015;162(5):974–986.

78. Wolff F, Leisch M, Greil R, Risch A, Pleyer L. The double-edged sword of (re)expression of genes by hypomethylating agents: from viral mimicry to exploitation as priming agents for targeted immune checkpoint modulation. *Cell Commun Signal*. 2017;15(1):13.

79. Robert C, Schachter J, Long GV, et al. Pembrolizumab versus Ipilimumab in Advanced Melanoma. *N Engl J Med*. 2015;372(26):2521–2532.

80. Larkin J, Chiarion-Sileni V, Gonzalez R, et al. Five-Year Survival with Combined Nivolumab and Ipilimumab in Advanced Melanoma. *N Engl J Med*. 2019;381(16):1535–1546.

81. Robert C, Ribas A, Hamid O, et al. Durable Complete Response After Discontinuation of Pembrolizumab in Patients With Metastatic Melanoma. *JCO*. 2018;36(17):1668–1674.

Table 1. Baseline patient characteristics

82. Heinhuis KM, Ros W, Kok M, et al. Enhancing antitumor response by combining immune checkpoint inhibitors with chemotherapy in solid tumors. *Annals of Oncology*. 2019;30(2):219–235.

83. Miller BC, Sen DR, Al Abosy R, et al. Subsets of exhausted CD8+ T cells differentially mediate tumor control and respond to checkpoint blockade. *Nat Immunol*. 2019;20(3):326–336.

84. Sade-Feldman M, Yizhak K, Bjorgaard SL, et al. Defining T Cell States Associated with Response to Checkpoint Immunotherapy in Melanoma. *Cell*. 2018;175(4):998-1013.e20.

85. Tirosh I, Izar B, Prakadan SM, et al. Dissecting the multicellular ecosystem of metastatic melanoma by single-cell RNA-seq. *Science (New York, N.Y.)*. 2016;352(6282):189.

86. Shallis RM, Bewersdorf JP, Gowda L, et al. Immune Checkpoint Inhibitor Therapy for Acute Myeloid Leukemia and Higher-Risk Myelodysplastic Syndromes: A Single-Center Experience. *Blood*. 2019;134(Supplement_1):1330.

87. Yang X, Ma L, Zhang X, Huang L, Wei J. Targeting PD-1/PD-L1 pathway in myelodysplastic syndromes and acute myeloid leukemia. *Experimental Hematology & Oncology*. 2022;11(1):11.

88. Mitroulis I, Tasis A, Grigoriou M, et al. Phenotypic and Molecular Landscape of Bone Marrow CD8+ T Cells in Myeloid Neoplasms Predicts Response to Treatment with Hypomethylating Agents. *Blood*. 2023;142(Supplement 1):4588.

Total No of patients, N	104
Age at diagnosis, N (%)	
>65yo	77 (74%)
<65yo	22 (21,2%)
N/A	5 (4,8%)
Sex, N (%)	
Male	69 (66.35%)
Female	35 (33.65%)
WHO classification, N (%)	
MDS-LB	19 (18.3%)
MDS-IB1	15 (14.4%)
MDS-IB2	26 (25.0%)
AML	32 (30.8%)
CMML-2	12 (11.5%)
Baseline blood counts, median (range)	
Hemoglobin (g/dL)	9.4 (5.4-14)
Absolute neutrophil count; ANC ($\times 10^9$/L)	2.01 (0-60)
Platelet count ($\times 10^9$/L)	90.5 (5-463)
(%) Bone marrow blasts, N (%)	
<5%	17 (16,4%)
5-10%	20 (19.2%)
11-20%	30 (28,85%)
>20%	30 (28,85%)
N/A	7 (6,7%)
Cytogenetic risk score (IPSS-R), N (%)	
Very good	3 (2,9%)
Good	57 (54,8%)

Intermediate	25 (24%)
Poor	2 (1,9%)
Very poor	9 (8,7%)
N/A	8 (7,7%)
Number of completed AZA cycles, median (range)	
HR-MDS	9 (1-59)
AML	7(1-70)
CMML-II	7 (3-36)
IPSS-R, N (%)	
Very low	4 (4.2%)
Low	8 (8.3%)
Intermediate	13 (13.6%)
High	30 (31.2%)
Very high	41 (42.7%)
IPSS-M, N (%)	
Very low	5 (5.2%)
Low	13 (13.6%)
Moderate low	5 (5.2%)
Moderate high	8 (8.3%)
High	21 (21.9%)
Very high	44 (45.8%)

Figure Legends

Figure 1. Untargeted analysis of CD45$^+$ immune cells in patients with MDS, AML and CMML by CyTOF. (**A**) Multidimensional scale plot depicting the relationship between bone marrow (BM) samples of patients with LR-MDS (n=12), HR-MDS (n=15), AML (n=16) and CMML (n=5). (**B**) UMAP displaying the major immune cell clusters. (**C**) Heatmap showing the expression of the markers used for the characterization of each cell cluster. (**D**) Box charts displaying the frequency of each cell cluster. (**E**) Violin plots showing the expression level of CXCR3 in the CD8 T1, CD8 T2 and CD4 T2 clusters, respectively. Kruskal Wallis followed by "two-stage" Benjamini, Krieger & Yekutieli multiple comparison test was used in D. One-way ANOVA followed by "two-stage" Benjamini, Krieger & Yekutieli multiple comparison test was used in E. *$p < 0.05$, **$p < 0.01$.

Figure 2. Identification of a CD8$^+$ subpopulation (CD57$^+$CXCR3$^+$) which distinguishes MDS patients from AML and CMML patients. (**A**) Representative viSNE plots, derived from the FlowSOM analysis of BM CD8$^+$ T cells from patients with LR-MDS (n=12), HR-MDS (n=15), AML (n=16) and CMML (n=5). (**B**) Bar plots displaying the proportion of the metaclusters between the groups, expressed as percentage within CD8$^+$ T cells. (**C**) Heatmap depicting the expression level of the T-related markers between the metaclusters. (**D**) Violin plots showing the expression level of CXCR3 in metacluster 1. (**E**) Representative flow cytometry plots for the identification of the CD57$^+$CXCR3$^+$ CD8$^+$ T cell subpopulation in a cohort of patients with LR-MDS (n=7), HR-MDS (n=27), AML (n=20) and CMML (n=10). (**F**) Percentage of CD57$^+$CXCR3$^+$ cells within CD8$^+$ T cells. Kruskal Wallis was used in B and D.

One-way ANOVA followed by "two-stage" Benjamini, Krieger, & Yekutieli multiple comparison test was used in F. *p< 0.05, **p < 0.01, ***p < 0.001.

Figure 3. Association between the frequency of CD57$^+$CXCR3$^+$CD8+ and outcome in patients with HR-MDS and AML under treatment with AZA. (**A**) Box plots displaying the percentage of the CD57$^+$CXCR3$^+$ cells within CD8+ T cells, assessed by flow cytometry in responders and non-responders (HR-MDS, n=12 Responders and 9 Non-Responders; AML, n=9 Responders and 11 Non-Responders; CMML, n=5 Responders and 5 Non-Responders). (**B**) After stratification of HR-MDS and AML patients to responders (n=12) and non-responders (n=19), FlowSOM analysis was performed on BM CD8$^+$ T cells, which generated 6 metaclusters that are projected onto the viSNE plots. Representative viSNE plots (one for each group) are shown. (**C**) Heatmap depicting the expression levels of all T-related markers (**D**) Box plots showing the proportion of all metaclusters, expressed as frequency within CD8$^+$ T cells. (**E**) Kaplan Meier curves for overall survival (OS) in patients which received AZA treatment, with ≤29% (n=51) and >29% (n=26) CD57$^+$CXCR3$^+$ CD8$^+$ T cells before treatment initiation. The survival curves were compared by Log-rank (Mantel-Cox) test and the p value is shown. Median OS of the ≤29% group was 20.98 months, while the median OS of the >29% group was 12.05 months. (**F**) Survival curves for each disease subgroup. Increased (%) CD57$^+$CXCR3$^+$ correlates significantly with worse survival in HR-MDS and AML patients, whereas no association is observed in CMML patients. (**G**) HR-MDS and AML patients with ≤29% CD57$^+$CXCR3$^+$ exhibited higher response rates. No association between the frequency of CD57$^+$CXCR3$^+$ CD8$^+$ T cells and response to therapy was observed in CMML patients. Unpaired Student's t test was used in A**.** Mann-Whitney U test was used in D. *p < 0.05, **p < 0.01, ***p < 0.001.

Figure 4. Profiling of BM-derived CD8$^+$ T cells of HR-MDS and AML patients with scRNA-seq. (**A**) Uniform Manifold Approximation and Projection (UMAP) of CD8$^+$ T cells identified 11 clusters. A total of 28,449 CD8$^+$ T cells were pooled from 4 HR-MDS (15,597 cells) and 5 AML patients (12,852 cells). (**B**) Bubble plot depicting the average expression of genes used to characterize the clusters. (**C**) Expression of selected genes projected onto UMAPs. (**D**) Heatmap showing selected top differentially expressed genes for each cell cluster. (**E**) Ridgeline plots displaying the cytotoxic signature score for each cell cluster, as defined by the expression of key-related genes. (**F**) Ridgeline plots displaying the cell cycle signature score for each cell cluster. Differential expression data are reported in Data sheet 1. (G) UMAP visualization of trajectories colored by pseudotime.

Figure 5. BM-derived CD8$^+$ T cells from responders (CR) to AZA show an enhanced ISG molecular signature compared to non-responders (FAIL) in scRNAseq analysis. (**A**) Comparison of separate UMAPs for CR (a total of 13,667 cells, 7,571 from MDS and 6,096 cells from AML patients, respectively) and FAIL patients (a total of 14,782 cells, 8,026 cells from MDS and 6,756 cells from AML patients, respectively). (**B**) Stacked bar chart showing the average distribution of clusters between the two groups. The percentage of cluster 10 (Proliferative) was increased in CR compared to FAIL patients (Unpaired Student's t test, p=0.0418). (**C**) Dot plot representing MSigDB (Hallmark 2020) enrichment analysis of positively enriched pathways in CR patients. Enriched pathways with a q-value <0.05 (Benjamini-Hochberg correction) are shown. (**D**) Gradient expression of representative selected genes involved in IFN-related pathways, as they are projected onto UMAPs. (**E**) ISG (Interferon Stimulated Genes) score of cluster 0 (*GZMK*) and violin plots showing the expression levels of

the top differentially expressed IFN-stimulated genes of cluster 0 (*GZMK*) between CR and FAIL. (**F**) ISG score of cluster 1 (*EOMES*) and violin plots showing the expression levels of the top differentially expressed IFN-stimulated genes of cluster 1 (*EOMES*) between CR and FAIL. (**G**) ISG score of cluster 2 (CTL_1) and violin plots displaying the expression levels of the top differentially expressed IFN-stimulated genes of cluster 2 (CTL_1) between CR and FAIL. (**H**) ISG score of cluster 4 (CTL_2) and violin plots displaying the expression levels of the top differentially expressed IFN-related genes of cluster 4 (CTL_2) between CR and FAIL. Differential expression data are reported in Data sheet 2.

Figure 6. BM-derived CD8$^+$ T cells of non-responders (FAIL) displayed suppressed cytotoxic molecular signature at the single-cell level. (**A**) Dot plot representing MSigDB (Hallmark 2020) enrichment analysis of positively enriched pathways in FAIL patients. Enriched pathways with a q-value <0.05 (Benjamini-Hochberg correction) are shown. (**B**) TGF-β signaling score of cluster 2 (CTL_1) and violin plots displaying the expression levels of the top differentially expressed genes of cluster 2 (CTL_1), involved in the enrichment of the TGF-β signaling pathway between CR and FAIL. (**C**) TGF-β signaling score of cluster 4 (CTL_2) and violin plots displaying the expression levels of the top differentially expressed genes of cluster 4 (CTL_2), involved in the enrichment of the TGF-β signaling pathway between CR and FAIL. (**D**) Comparison of the cytotoxic score of each group, as it is projected onto the respective UMAPs. (**E**) Cytotoxic score of cluster 2 (CTL_1) and violin plots exhibiting the expression levels of the top differentially expressed cytotoxicity-related genes of cluster 2 (CTL_1) between CR and FAIL. (**F**) Cytotoxic score of cluster 4 (CTL_2) and violin plots exhibiting the

expression levels of the top differentially expressed cytotoxicity-related genes of cluster 4 (CTL_2) between CR and FAIL. Differential expression data are reported in Data sheet 2.

Figure 7. Transcription Factor (TF) regulatory network analysis in BM-derived CD8$^+$ T cells. (**A**) UMAP depicting the clustering of CD8$^+$ T cells based on regulons. (**B**) Pie charts illustrating the representation of cells from CR and FAIL patients within each regulon. (**C**) Comparison of cell distribution in regulons between the groups utilizing separate UMAPS for each group. (**D**) Heatmap showing the top differentially activated TFs of each regulon-cluster. (**E-F**) Violin plots depicting the activity score of selected TFs per sample type in regulons 5 and 7, respectively.

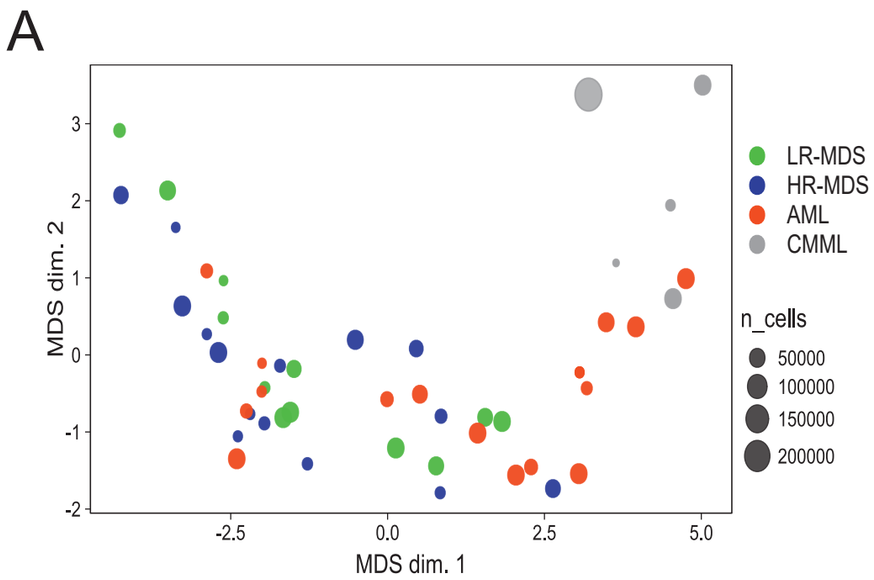
A
MDS dim. 2
MDS dim. 1
LR-MDS
HR-MDS
AML
CMML
n_cells
50000
100000
150000
200000

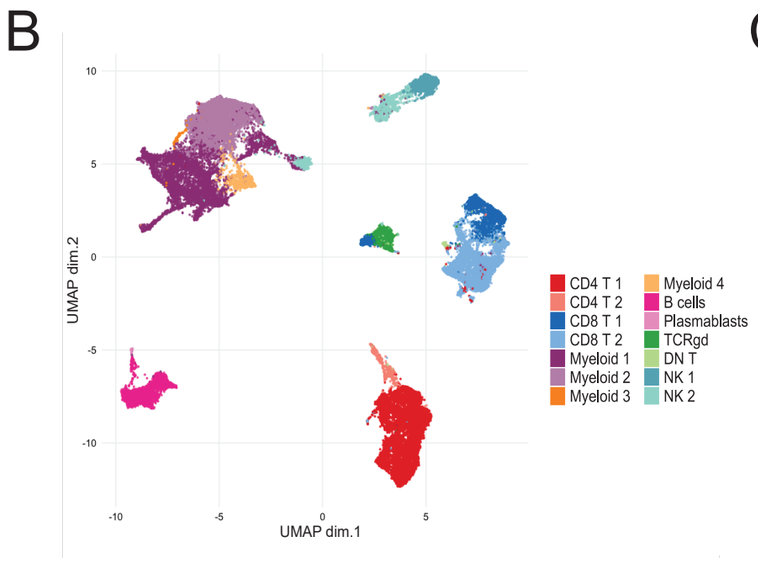
B
UMAP dim.2
UMAP dim.1
CD4 T 1
CD4 T 2
CD8 T 1
CD8 T 2
Myeloid 1
Myeloid 2
Myeloid 3
Myeloid 4
B cells
Plasmablasts
TCRgd
DN T
NK 1
NK 2

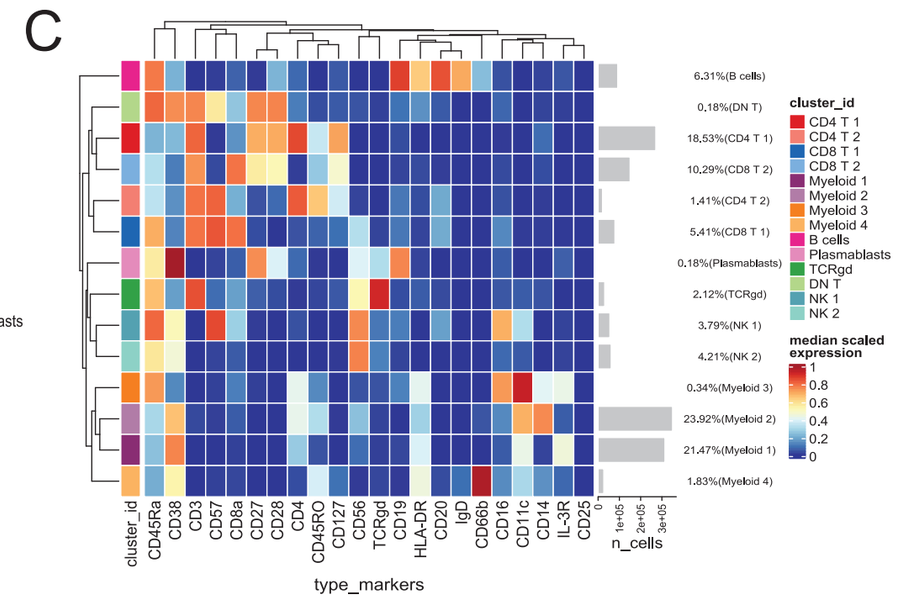
C
6.31%(B cells)
0.18%(DN T)
18.53%(CD4 T 1)
10.29%(CD8 T 2)
1.41%(CD4 T 2)
5.41%(CD8 T 1)
0.18%(Plasmablasts)
2.12%(TCRgd)
3.79%(NK 1)
4.21%(NK 2)
0.34%(Myeloid 3)
23.92%(Myeloid 2)
21.47%(Myeloid 1)
1.83%(Myeloid 4)
cluster_id
CD4 T 1
CD4 T 2
CD8 T 1
CD8 T 2
Myeloid 1
Myeloid 2
Myeloid 3
Myeloid 4
B cells
Plasmablasts
TCRgd
DN T
NK 1
NK 2
median scaled expression
cluster_id
CD45Ra
CD38
CD3
CD57
CD8a
CD27
CD28
CD4
CD45RO
CD127
CD56
TCRgd
CD19
HLA-DR
CD20
IgD
CD66b
CD16
CD11c
CD14
IL-3R
CD25
n_cells
type_markers

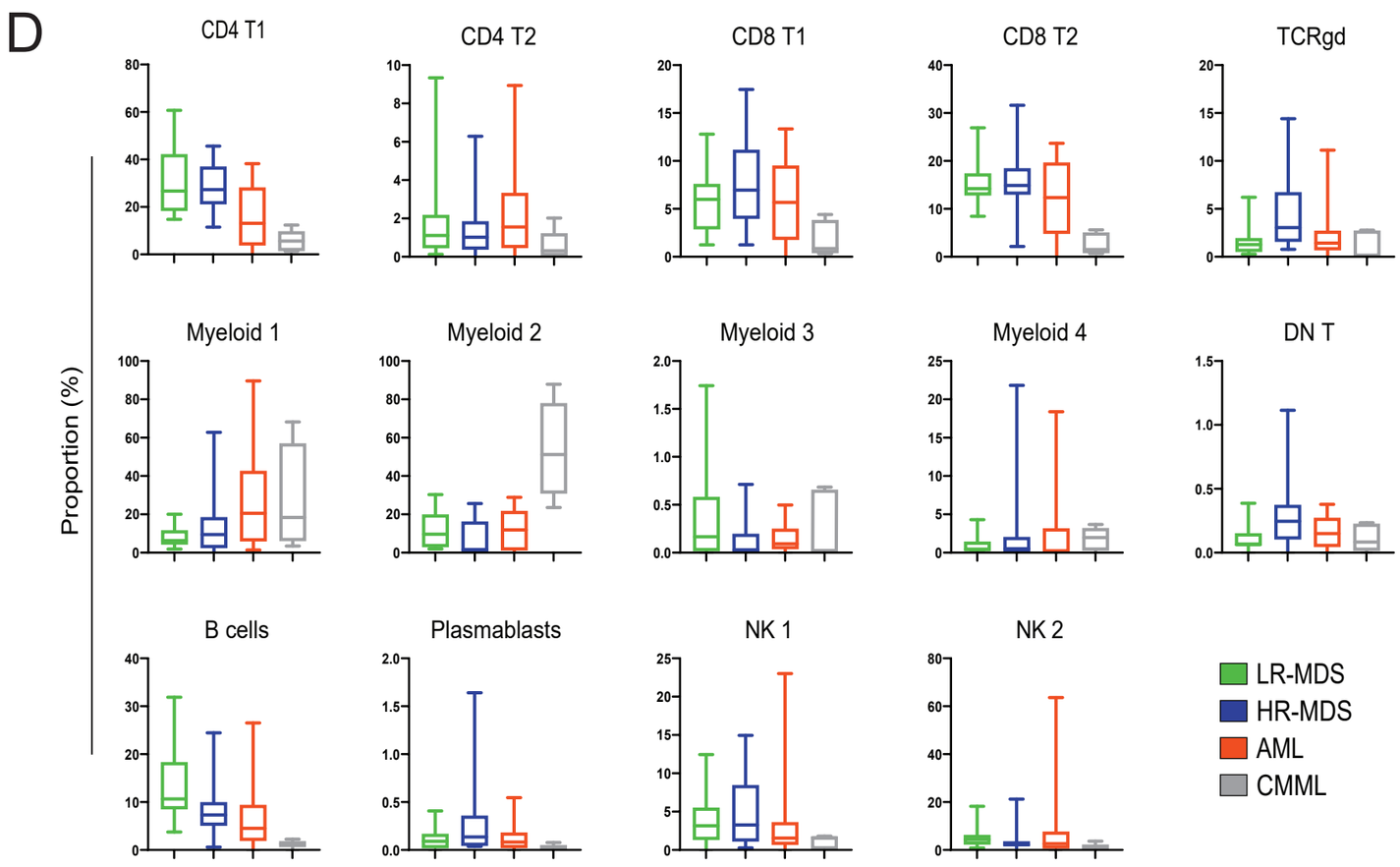
D
CD4 T1
CD4 T2
CD8 T1
CD8 T2
TCRgd
Myeloid 1
Myeloid 2
Myeloid 3
Myeloid 4
DN T
B cells
Plasmablasts
NK 1
NK 2
Proportion (%)
LR-MDS
HR-MDS
AML
CMML

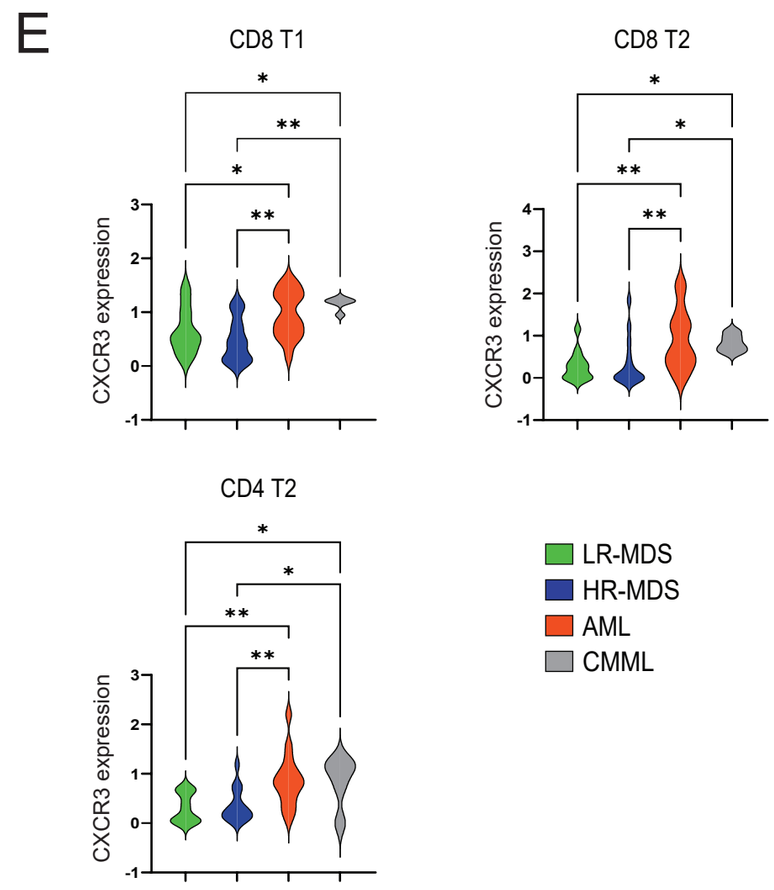
E
CD8 T1
CD8 T2
CD4 T2
CXCR3 expression
LR-MDS
HR-MDS
AML
CMML

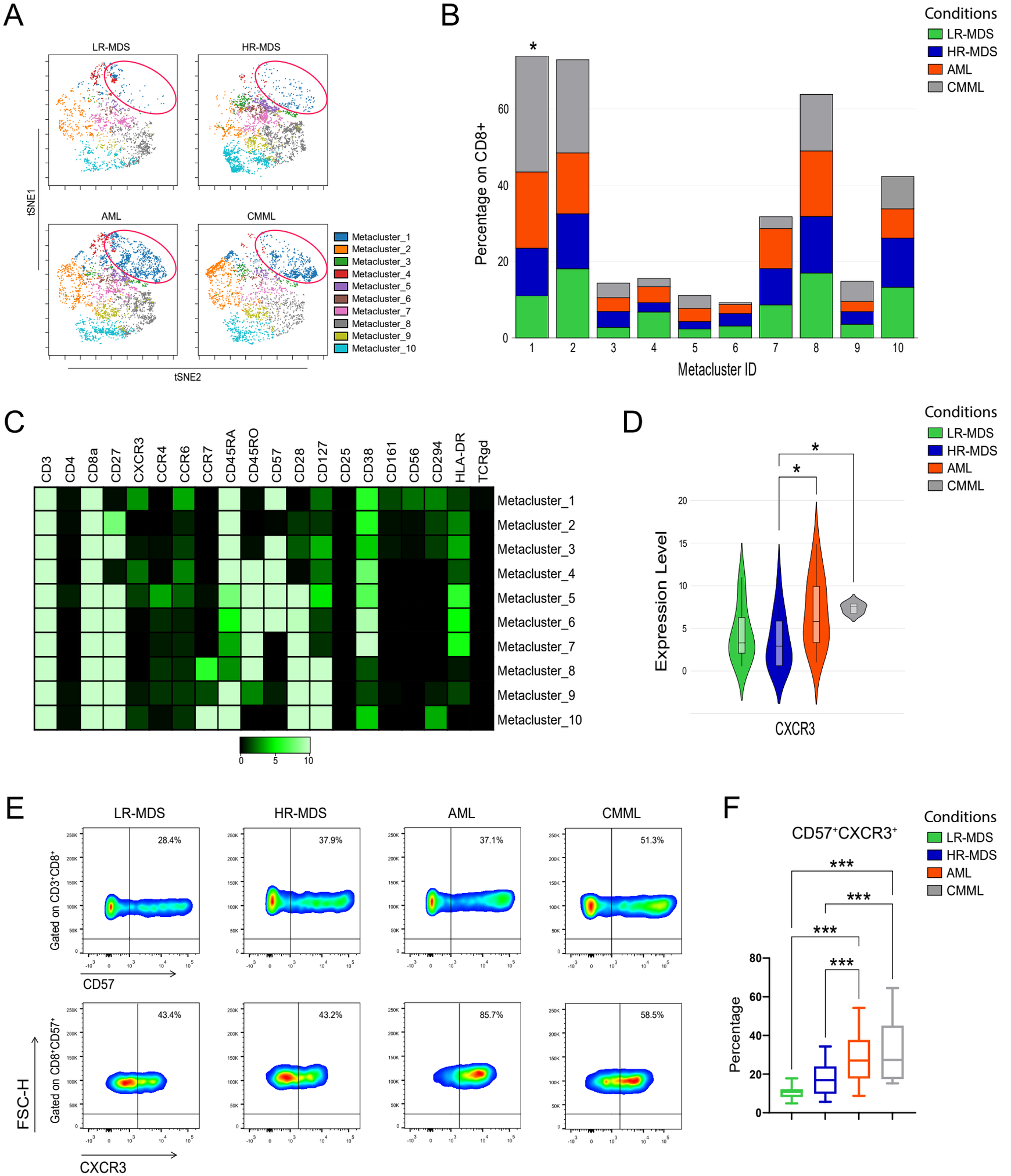
A
LR-MDS
HR-MDS
AML
CMML
tSNE1
tSNE2
Metacluster_1
Metacluster_2
Metacluster_3
Metacluster_4
Metacluster_5
Metacluster_6
Metacluster_7
Metacluster_8
Metacluster_9
Metacluster_10
B
Conditions
LR-MDS
HR-MDS
AML
CMML
Percentage on CD8+
Metacluster ID
C
CD3
CD4
CD8a
CD27
CXCR3
CCR4
CCR6
CCR7
CD45RA
CD45RO
CD57
CD28
CD127
CD25
CD38
CD161
CD56
CD294
HLA-DR
TCRgd
D
Expression Level
CXCR3
E
Gated on CD3+CD8+
CD57
Gated on CD8+CD57+
CXCR3
FSC-H
28.4%
37.9%
37.1%
51.3%
43.4%
43.2%
85.7%
58.5%
F
CD57+CXCR3+
Percentage

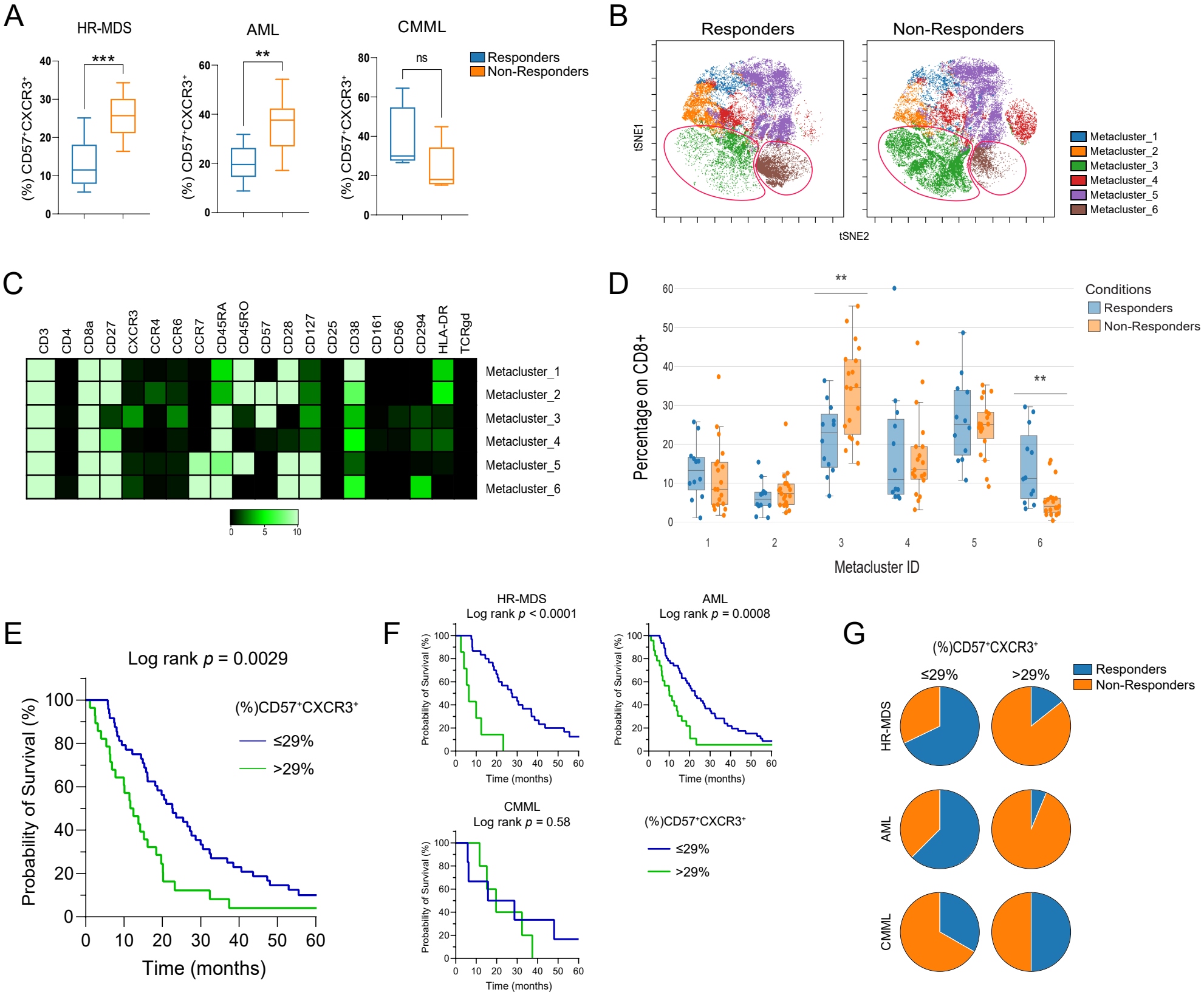
A
HR-MDS
AML
CMML
***
**
ns
(%) CD57+CXCR3+
Responders
Non-Responders
B
Responders
Non-Responders
tSNE1
tSNE2
Metacluster_1
Metacluster_2
Metacluster_3
Metacluster_4
Metacluster_5
Metacluster_6
C
CD3
CD4
CD8a
CD27
CXCR3
CCR4
CCR6
CCR7
CD45RA
CD45RO
CD57
CD28
CD127
CD25
CD38
CD161
CD56
CD294
HLA-DR
TCRgd
Metacluster_1
Metacluster_2
Metacluster_3
Metacluster_4
Metacluster_5
Metacluster_6
D
Percentage on CD8+
Metacluster ID
Conditions
Responders
Non-Responders
E
Log rank p = 0.0029
(%)CD57+CXCR3+
≤29%
>29%
Probability of Survival (%)
Time (months)
F
HR-MDS
Log rank p < 0.0001
AML
Log rank p = 0.0008
CMML
Log rank p = 0.58
Probability of Survival (%)
Time (months)
(%)CD57+CXCR3+
≤29%
>29%
G
(%)CD57+CXCR3+
≤29%
>29%
Responders
Non-Responders
HR-MDS
AML
CMML

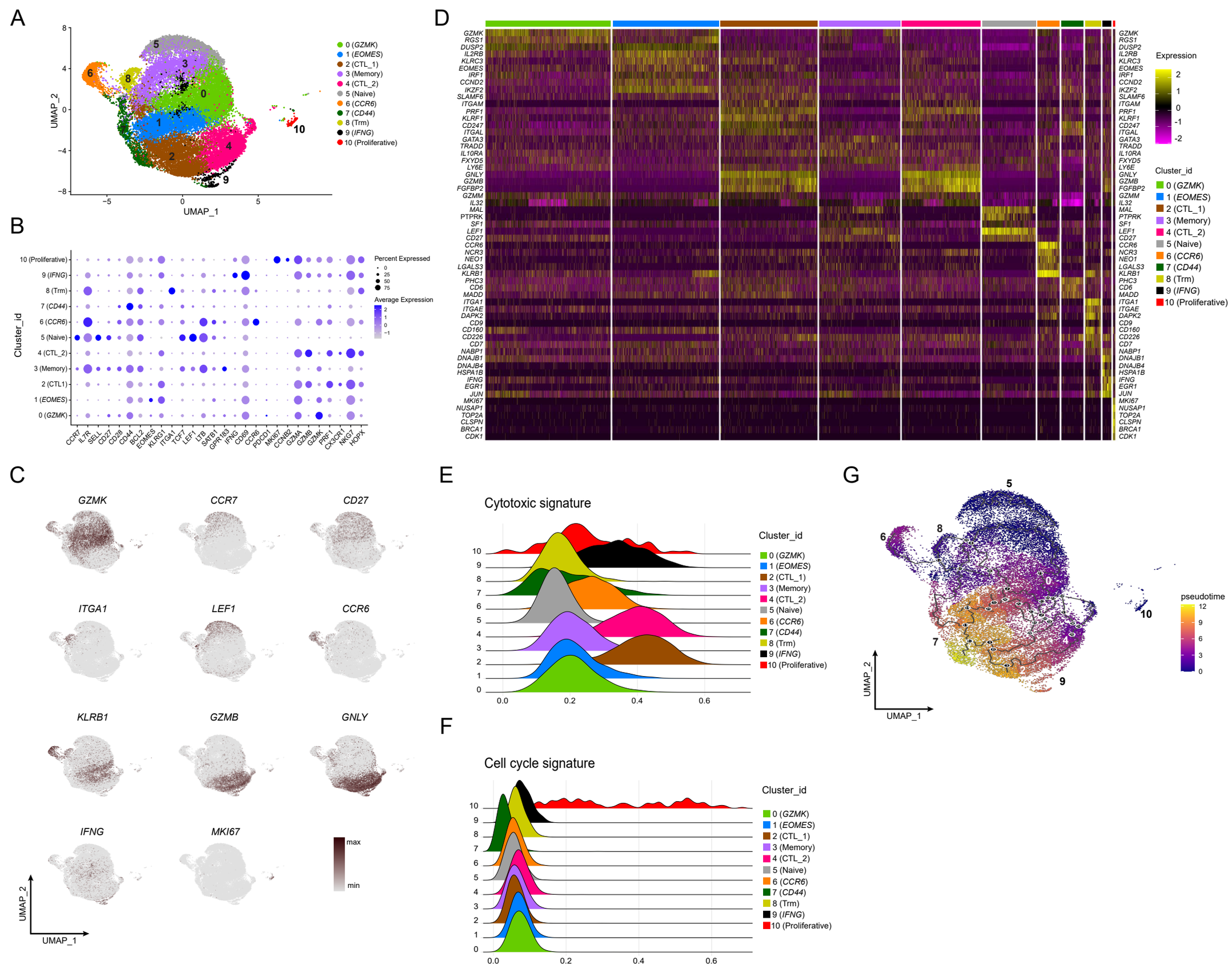
A
UMAP_2
UMAP_1
0 (GZMK)
1 (EOMES)
2 (CTL_1)
3 (Memory)
4 (CTL_2)
5 (Naive)
6 (CCR6)
7 (CD44)
8 (Trm)
9 (IFNG)
10 (Proliferative)
B
Cluster_id
Percent Expressed
Average Expression
CCR7 IL7R SELL CD27 CD28 CD44 BCL2 EOMES KLRG1 ITGA1 TCF7 LEF1 LTB SATB1 GPR183 IFNG CD69 CCR6 PDCD1 MKI67 CCNB2 GZMA GZMB GZMK PRF1 CX3CR1 NKG7 HOPX
C
GZMK
CCR7
CD27
ITGA1
LEF1
CCR6
KLRB1
GZMB
GNLY
IFNG
MKI67
max
min
UMAP_2
UMAP_1
D
Expression
Cluster_id
GZMK RGS1 DUSP2 IL2RB KLRC3 EOMES IRF1 CCND2 IKZF2 SLAMF6 ITGAM PRF1 KLRF1 CD247 ITGAL GATA3 TRADD IL10RA FXYD5 LY6E GNLY GZMB FGFBP2 GZMM IL32 MAL PTPRK SF1 LEF1 CD27 CCR6 NCR3 NEO1 LGALS3 KLRB1 PHC3 CD6 MADD ITGA1 ITGAE DAPK2 CD9 CD160 CD226 CD7 NABP1 DNAJB1 DNAJB4 HSPA1B IFNG EGR1 JUN MKI67 NUSAP1 TOP2A CLSPN BRCA1 CDK1
E
Cytotoxic signature
Cluster_id
F
Cell cycle signature
Cluster_id
G
pseudotime
UMAP_2
UMAP_1

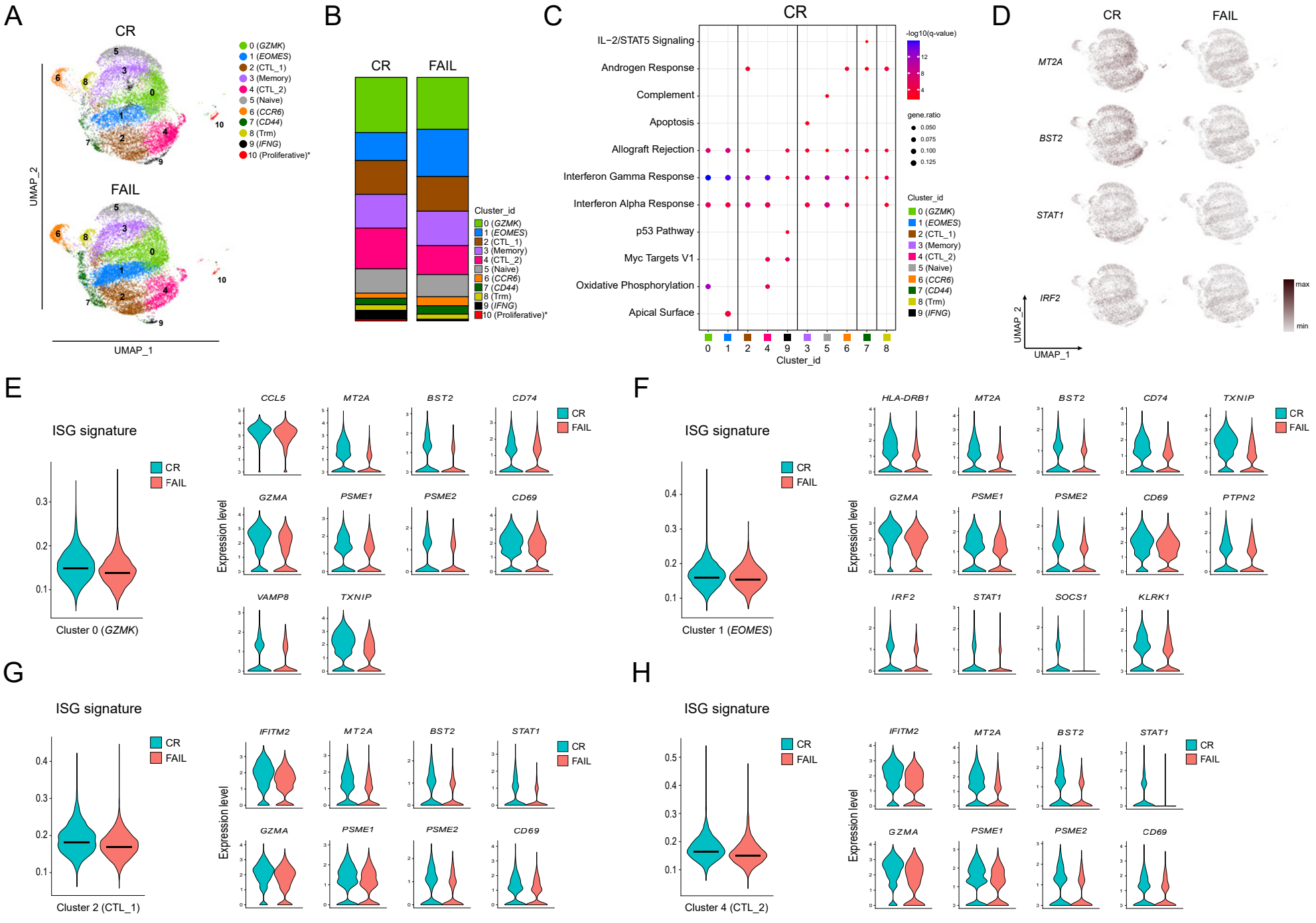
A
CR
FAIL
UMAP_1
UMAP_2
0 (GZMK)
1 (EOMES)
2 (CTL_1)
3 (Memory)
4 (CTL_2)
5 (Naive)
6 (CCR6)
7 (CD44)
8 (Trm)
9 (IFNG)
10 (Proliferative)*
B
CR
FAIL
Cluster_id
C
CR
IL−2/STAT5 Signaling
Androgen Response
Complement
Apoptosis
Allograft Rejection
Interferon Gamma Response
Interferon Alpha Response
p53 Pathway
Myc Targets V1
Oxidative Phosphorylation
Apical Surface
-log10(q-value)
gene.ratio
Cluster_id
D
CR
FAIL
MT2A
BST2
STAT1
IRF2
max
min
E
ISG signature
CR
FAIL
Cluster 0 (GZMK)
Expression level
CCL5
MT2A
BST2
CD74
GZMA
PSME1
PSME2
CD69
VAMP8
TXNIP
F
ISG signature
Cluster 1 (EOMES)
HLA-DRB1
TXNIP
PTPN2
IRF2
STAT1
SOCS1
KLRK1
G
ISG signature
Cluster 2 (CTL_1)
IFITM2
H
ISG signature
Cluster 4 (CTL_2)

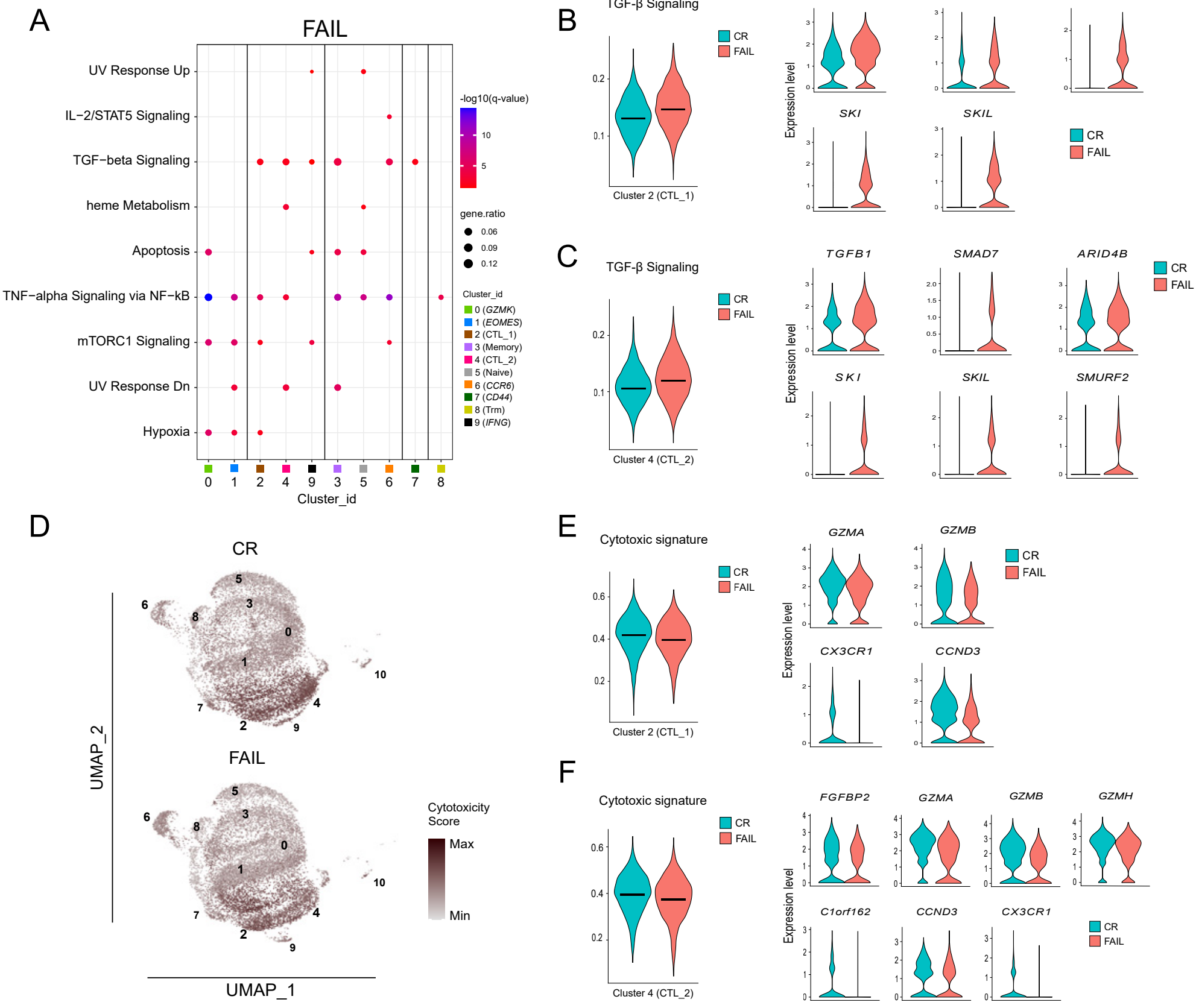
A
FAIL
UV Response Up
IL−2/STAT5 Signaling
TGF−beta Signaling
heme Metabolism
Apoptosis
TNF−alpha Signaling via NF−kB
mTORC1 Signaling
UV Response Dn
Hypoxia
-log10(q-value)
10
5
gene.ratio
0.06
0.09
0.12
Cluster_id
0 (GZMK)
1 (EOMES)
2 (CTL_1)
3 (Memory)
4 (CTL_2)
5 (Naive)
6 (CCR6)
7 (CD44)
8 (Trm)
9 (IFNG)
0 1 2 4 9 3 5 6 7 8
Cluster_id
B
TGF-β Signaling
CR
FAIL
Cluster 2 (CTL_1)
Expression level
TGFB1
SMURF2
SMAD7
SKI
SKIL
C
TGF-β Signaling
Cluster 4 (CTL_2)
ARID4B
D
CR
FAIL
UMAP_2
UMAP_1
Cytotoxicity Score
Max
Min
E
Cytotoxic signature
GZMA
GZMB
CX3CR1
CCND3
F
FGFBP2
GZMH
C1orf162

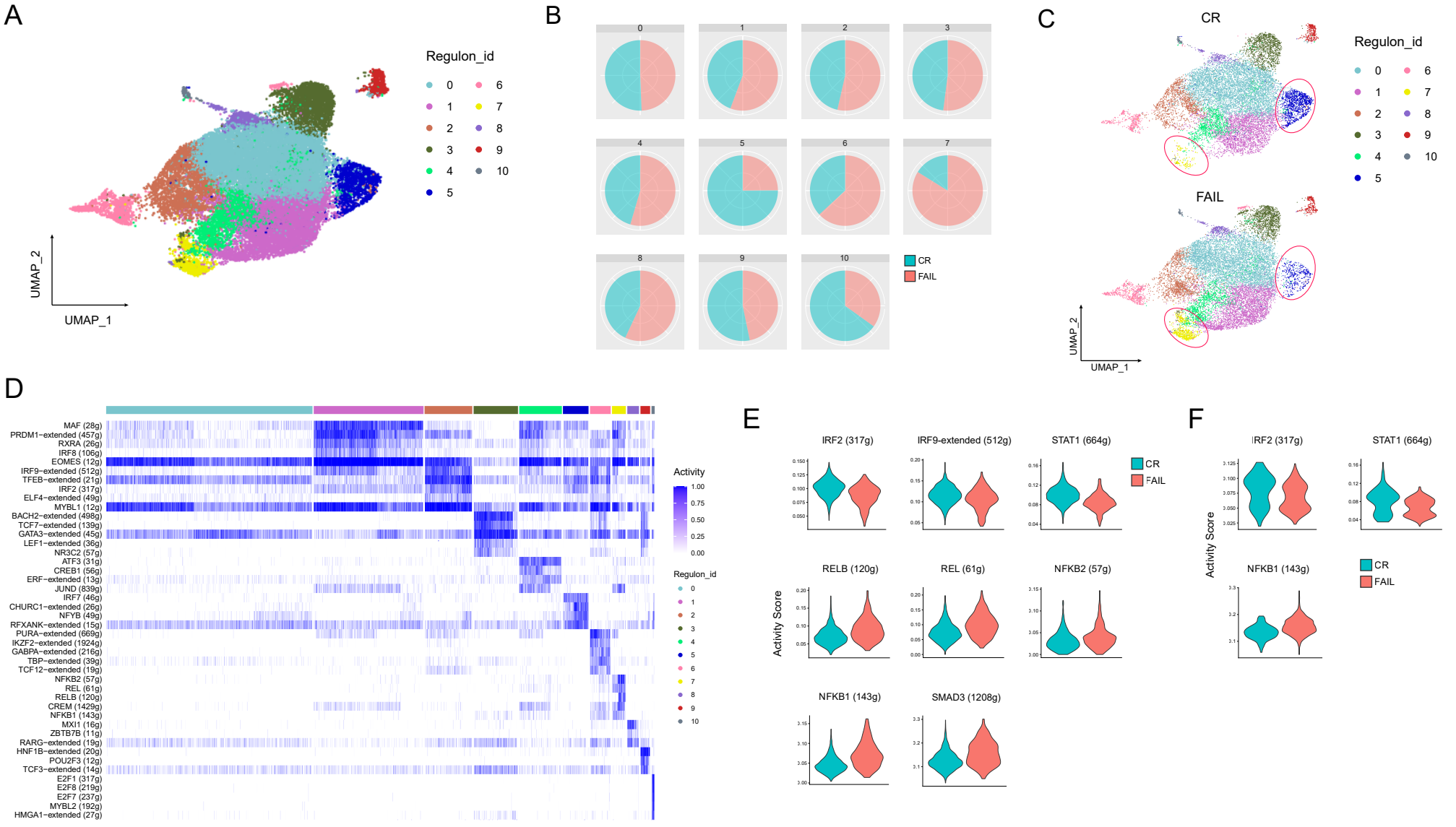
A
Regulon_id
0
1
2
3
4
5
6
7
8
9
10
UMAP_2
UMAP_1
B
CR
FAIL
C
CR
FAIL
D
MAF (28g)
PRDM1−extended (457g)
RXRA (26g)
IRF8 (106g)
EOMES (12g)
IRF9−extended (512g)
TFEB−extended (21g)
IRF2 (317g)
ELF4−extended (49g)
MYBL1 (12g)
BACH2−extended (498g)
TCF7−extended (139g)
GATA3−extended (45g)
LEF1−extended (36g)
NR3C2 (57g)
ATF3 (31g)
CREB1 (56g)
ERF−extended (13g)
JUND (839g)
IRF7 (46g)
CHURC1−extended (26g)
NFYB (49g)
RFXANK−extended (15g)
PURA−extended (669g)
IKZF2−extended (1924g)
GABPA−extended (216g)
TBP−extended (39g)
TCF12−extended (19g)
NFKB2 (57g)
REL (61g)
RELB (120g)
CREM (1429g)
NFKB1 (143g)
MXI1 (16g)
ZBTB7B (11g)
RARG−extended (19g)
HNF1B−extended (20g)
POU2F3 (12g)
TCF3−extended (14g)
E2F1 (317g)
E2F8 (219g)
E2F7 (237g)
MYBL2 (192g)
HMGA1−extended (27g)
Activity
1.00
0.75
0.50
0.25
0.00
Regulon_id
E
IRF2 (317g)
IRF9-extended (512g)
STAT1 (664g)
RELB (120g)
REL (61g)
NFKB2 (57g)
NFKB1 (143g)
SMAD3 (1208g)
Activity Score
CR
FAIL
F
IRF2 (317g)
STAT1 (664g)
NFKB1 (143g)
Activity Score
CR
FAIL